Collapse and damage to vernacular buildings induced by 2012 Emilia earthquakes

Published Version:
Bovo, M., Barbaresi, A., Torreggiani, D., Tassinari, P. (2020). Collapse and damage to vernacular buildings induced by 2012 Emilia earthquakes. BULLETIN OF EARTHQUAKE ENGINEERING, 18(3), 1049-1080 [10.1007/s10518-019-00737-7].

Availability:
This version is available at: https://hdl.handle.net/11585/737298 since: 2024-11-14

Published:
DOI: http://doi.org/10.1007/s10518-019-00737-7

(Article begins on next page)

Collapse and damage to vernacular buildings induced by 2012 Emilia earthquakes

Bovo Marco[1,*], Barbaresi Alberto[1], Torreggiani Daniele[1] and Tassinari Patrizia[1]

Abstract

In May 2012, two seismic events hit the Emilia-Romagna Region, in Northern Italy. The earthquakes caused collapses and damage to traditional vernacular building heritage, highlighting its seismic high vulnerability. The paper presents a wide collection of damage and collapses observed in the aftermath field inspections on 22 historical vernacular buildings. It was noted that few recurring structural typologies are present in the area hit by earthquake and buildings of the same typology show similar damage mechanisms. Then, with the main goal to identify the most typical damage affecting similar structures, the building stock has been subdivided in different categories based on building plan distribution and intended use. The principal collapse causes, based both on in-field observations and analyses, performed on local and global finite element models, can be ascribed to poor connections between orthogonal walls, lack of effective connections between floor elements and walls, excessive flexibility of floor diaphragms and high slenderness of vertical elements. The outcomes in the present paper allow identifying the vernacular building typologies most vulnerable to earthquake and can help to plan the future retrofitting strategies for vernacular heritage.

Keywords: vernacular building; masonry building; rural heritage; seismic damage; local mechanism; Emilia earthquake

[1] DISTAL - University of Bologna, Viale G. Fanin 48, 40127 Bologna (BO) - Italy
* **Corresponding author** – Email: marco.bovo@unibo.it

1. Introduction

More than 1,000 seismic events with magnitude bigger than 2.0 [1] hit, in May 2012, the Emilia-Romagna, Lombardia and Veneto Regions located in the North of Italy. Two main earthquakes, with very close epicentres (about 12 km of distance) characterized the sequence named Emilia Earthquake. The first main shock of May 20 (epicentre latitude and longitude 44.89N and 11.23E, respectively) had local magnitude equal to 5.9 and peak ground acceleration (PGA) of 258.80 cm/s^2 (i.e. 0.26g). For the second main shock of May 29 (epicentre latitude and longitude 44.85N and 11.09E, respectively), the local magnitude was 5.8 and PGA=411.37 cm/s^2 (i.e. 0.42g) [2]. Figure 1 shows the shake maps extracted by [2] for the two close-range earthquakes.

The areas shaken by the earthquakes are moderately populated (from 50 to 300 inhabitants/km^2). They are characterized by small residential centres and medium-sized productive areas, surrounded by rural landscapes. Headquarters of some of the most important Italian brands (food production, automotive, etc.) are located in this area, making this region one of the most densely industrialized and most productive of the North of the country [3]. Several collapses and extended damage occurred, involving precast reinforced concrete (RC) industrial structures [4]-[6], masonry monumental heritage [7]-[9] and historical rural buildings [10]-[11], highlighting that vernacular buildings represent one of the most vulnerable categories of a region where the agricultural activities play a fundamental role for the economy of the territory.

The first earthquake heavily damaged the areas of San Carlo di Sant'Agostino, Mirabello, Finale Emilia, and San Felice sul Panaro (Modena and Ferrara Provinces, Emilia-Romagna). The second main shock caused collapses in the areas of Mirandola, Medolla, Cavezzo, Novi di Modena, and Moglia (Modena and Ferrara Provinces, Emilia-Romagna). In the aftermath of the earthquakes, spread soil liquefaction phenomena have been observed close to epicentres. By processing the outcomes of the building surveys activated immediately after the sequence, about 25% of residential buildings and 45% of industrial facilities turned out to be unsafe and were condemned, due to the reported significant damage or failures [12].

The main reason of vernacular building collapses must be attributed to an incorrect design philosophy, typical of past construction techniques in non-seismic zones, that consider gravitational and wind loads only. The Emilia area, in fact, was considered non-seismic zone until 2003, therefore most of the buildings hit by the earthquake were designed without seismic details. Moreover, old rural buildings were often realized with poor construction techniques and low-quality materials as emerged by the experimental tests widely described in several works [13]-[16]. The commonly observed collapses were wall local mechanisms (i.e. single or complex overturning, horizontal flexure and vertical flexure) and, in some cases, in-plane shear of flexure failures. In few cases, the irregular distribution of masonry infill panels in between consecutive masonry columns, anticipated the failure.

The failures must be ascribed to the lack of effective connections between orthogonal walls, poor connections between floor elements and walls, excessive flexibility of floor diaphragms and high vertical elements slenderness.

With regard to historical vernacular buildings, few recurrent typologies are present in the areas hit by the earthquake. Moreover, buildings of the same typology showed similar damage mechanisms. Therefore, even though every structure has its own features, it is possible to subdivide the vernacular buildings of Emilia territories into few categories with same intended use, and then connect the categories to recurrent damage mechanisms. This allows identifying the most vulnerable building categories (or typologies) and, from the lesson learned after the seismic events, to design the future strategies necessary to increase the safety of ancient rural constructions. Under this light, some researchers focused their attention on the study of the seismic vulnerabilities of vernacular buildings [17] [18] in order to address the most important deficiencies [19] and to evaluate earthquake resistant solutions aimed at increasing the capacity of these constructions [20]. Vernacular buildings, as much as historical monumental constructions, currently represent a large cultural heritage, marking the architectural, environmental and social features of landscape. On the other side, despite their importance, specific laws or regulations aimed at their preservation are nowadays not in effect and several of these buildings are abandoned and in advanced deterioration state [21].

The work presents and describes a wide collection of damage and collapses observed in the aftermath in-field inspections on 22 historical vernacular buildings. During the building surveys, the main features of the historical vernacular building heritage of the region were identified and collected. Therefore, in order to define the damage mechanisms affecting similar structures, the stock has been subdivided in five different categories based on plan distribution and use. In general, the main damage/collapse causes can be ascribed poor connections between orthogonal walls, lack of effective connections between floor elements and walls, excessive flexibility of floor diaphragms and high vertical walls slenderness. In detail, for each structural category, the collapse mechanisms are identified, and the main failures causes are discussed. In order to proof the outcomes from the in-field observations, a comparison with the results coming from numerical analyses performed on different (global and local) finite element models were set. The analyses of the collapse described in the paper provide a better understanding of the seismic vulnerabilities of vernacular buildings necessary to propose the most effective retrofitting interventions.

2. Preliminary considerations on May 2012 earthquakes

In this section some aspects related to the ground motions shaking northern Italy in May of 2012 will be introduced. Table 1 reports some useful data on the main shocks recorded by some accelerometric stations sited close to the epicentres. The positions of the stations are showed in Figure 1, together with the epicentres and building stock under study in this paper. As stated in Introduction, two earthquakes with analogous magnitude were recorded in a short time (i.e. 9 days) and short geographical distance (around 11.9km). This represents a very rare event, even rarer considering that the event of May 29th is not on the same fault plane as the May 20th event, but seems just to have a seismic source with analogous characteristics. In fact, the analysis of the slip model exhibited that the two shocks have distinct and separate slip sources with possible separate fault planes [22]. Following the actual Italian seismic hazard map [23], the maximum PGA value recorded for the second main shock (i.e. 0.42g) is comparable to expected value for a very rare seismic event. The pseudo-acceleration response spectra, for both the events, are showed in Figure 3, for records in a range of about 40 km. It is worth noticing that during the second shock, a larger number of monitoring instruments was used, meaning that more stations recorded the events. Thanks to this, a deeper comprehension of the near source effects on the area was possible. In fact, high vertical acceleration and pulse-like characteristics can be observed in a few records. These effects could play a relevant role in the damage state of buildings in the proximity of an epicentre, since, typically, near-fault ground motions have bigger destructive potential than far-fault [24]-[26].

The elastic pseudo-acceleration response spectra of vertical ground motion records are reported in Figure 4. During the second event the station MRN, located 4.1 km far from the epicentre position, recorded a PGA_V of about 0.86g (i.e. 840.74cm/s^2). The PGA_V recorded 18 km far from the epicentre was about 0.19g (i.e. 189.07cm/s^2 for the station SAN0 in Table 1), equivalent to 20% of the maximum recorded. A similar line on reasoning on PGA_H leads to define a percentage ratio of 57%, between the PGA_H recorded 18km from the epicentre and the maximum value registered. This confirms that also for the Emilia sequence the vertical acceleration has near field features and, as expected [22], vertical acceleration attenuates faster over the distance than horizontal one. Furthermore, the comparison between Figure 3 and 4 shows that spectral amplifications in vertical direction involve short vibrating periods, resulting in accelerations nearly negligible for structures with vertical periods longer than 0.3s. In a following Section, it will be shown that vertical vibrating period of traditional rural buildings is typically longer than 0.3s, and probably the vertical accelerations played a marginal role in the seismic-induced observed damage for this class of buildings. On the contrary, for existing precast RC buildings, having shorter vertical vibrating periods ranging from 0.1s to 0.4s [27], the presence of vertical accelerations resulted decisive to explain many collapses. Differently from the vertical ones, the horizontal pseudo-acceleration spectra present the maximum ordinates in the typical range of some vernacular building typologies studied here.

As for other features of the investigated sequence, it is worth to highlight that site response effect proposed by Priolo et al. [28] was confirmed by Gallipoli et al. [29], explaining the large acceleration demand showed by the spectra of the ground motions recorded on May 29th by the station MIR01, very close to the epicentre. Several damage observed on rural structures can be strongly related to the peak acceleration response spectra since the peak is located exactly on the vibrating periods' range of some building categories studied in this work (see the next Section). Furthermore, in addition to local site effects, some of the records of May 29th present near-fault characteristics like directivity and pulse-like effects [30]. Then, as widely confirmed by literature review, pulse-like seismic inputs lead to larger inelastic displacement demands if compared to non-pulse-like ground-motions, and could cause greater residual story displacements on the structures [31]-[32]. To this regard, the maps of Figure 5 show, for the investigated area, the curves of the peak relative displacement for the two events as obtained by applying the records on a single degree of freedom (SDOF) elastic system. In Figure 5a and c the results for a SDOF with period of 0.3s are presented, while in Figure 5b and d the period is 1.0s. For short periods the displacement demand reaches maximum values of 5-6cm, while, for more flexible buildings, values of 20-25cm were assessed in proximity of the epicentres. The considerable displacement values, expected in case of flexible structures, could represent a cause of collapse. In fact, the large displacements can activate wall local mechanisms and, in absence of devices able to prevent the sliding of wooden beams from vertical elements typical of poor vernacular buildings of the Emilia territory, induce the fall of roof elements due to the reduced support length.

3. Vernacular building heritage in the region

3.1 Main characteristics of the historical vernacular settlements

Currently, according to the last ISTAT census [21], in the municipalities of the area hit by the earthquake, most of the structures are two-storey masonry buildings. Rural buildings represent a relevant percentage of the whole stock of the Emilia-Romagna Region. The Po valley area, stricken by the earthquakes, has similar vocations (mainly because of the local geography) and most of the historical vernacular buildings have been built in a short time period of about 150 years (i.e. during the 19th century and the first half of the 20th century). In fact, most of the rural dwellings built before the 19th century were made up with natural perishable materials (e.g. mud, straws, wood, canes and raw bricks), and after World War II the modification of socio-economic conditions soon imposed new building typologies and more efficient technologies (i.e. RC or steel precast elements). Albeit every structure has its own geometry, dimensions, architectural arrangement and inner distribution, the vernacular building heritage of the area is quite homogeneous and constituted by few typologies [33]. Based on an historical research, Ortolani [34] describes the typical rural courtyard of the area of Modena as depicted in Figure 6a. The main buildings of a settlement are: (i) the residential house, having rectangular shape and basic rooms (usually with kitchen, warehouse, and basement at the ground floor; bedrooms and a little granary at the first floor), (ii) the stable-hayloft, and (iii) some buildings used for minor services (i.e. toilet shack, garage, henhouse, etc.). This description is still valid and faithfully represents the distribution of the rural settlements in the territory. Often house and stable-hayloft were built one adherent to the other, with an internal common wall as separation. In other cases, maybe more typical of the countryside surrounding the Reggio Emilia Province, the two buildings are connected by a transition element, the "porta morta" (i.e. blind door). This characteristic element is depicted in detail in Figure 6b. The "porta morta" represented a protected passage where the peasants get undressed before entering the house, and sometimes was used to collect and dry spices and little quantity of cereals. The volume was typically open with a masonry arch on the front side, and closed by walls on the back, this giving the origin to the name. In some buildings the "porta morta" is opened on both the façades. Even in this case, from a structural point of view, the two buildings are connected and then the dynamic behaviour of the whole system depends from the characteristics of the connections between the walls of the "porta morta" volume and the walls of the lateral bodies.

Typically, few smaller buildings were dedicated to minor services. The largest farms had some further buildings, which in the past were used to store large quantities of hay, and more recently were used to store agricultural tools and equipment. With reference to this last building class, the most spread typologies are the "barchessa" and the "casella". Following the traditional definition in [34], the "barchessa" was vertically closed by perimeter walls on three façades, while the original "casella" has just one or two closed façades and is open on the others, where columns are present. They appear as a wide portico sustained by very slender columns or walls.

3.2 Classification criteria and description of the building stock

In the aftermath on-field damage surveys in the area hit by the earthquakes, the authors collected the documentation of 22 historical vernacular buildings, damaged or collapsed during the earthquakes. The main characteristics of the building stock of this paper are summarized in Table 2 and Table 3, while the position of each building (abbreviated bldg. in figure and table captions) is reported in Figure 1.

For the classification and subdivision of the building stock of this study, two basic criteria were adopted. The first refers to geometry and plan distribution of the building, the second to the building use. Following the first criterion, buildings are considered isolated when structurally not connected to other bodies (A), or composed, when made up of several structurally connected bodies (B). According to the second criterion, we have: dwellings for residential use (1), stable-haylofts (2), “barchessa” or “casella” constructions (3) and buildings used for other minor services (4).

In the building stock, there are 17 isolated buildings (i.e. 6 A1 + 4 A2 + 2 A3 + 5 A4) and 5 composed buildings (i.e. 4 B1-2 + 1 B1-4). The epicentre-building distance lies in the ranges 5-34 km for the first main shock and 3-29 km for the second shock.

During the inspections it has been observed that, typically, the buildings of category A1 have 25-30 cm thick masonry walls made up with irregular raw bricks and poor hydraulic mortar brickworks (see Figure 7a), 2.50-2.80 m net floor height and no more than three floors. The intermediate floors are built with timber beams (e.g. see Figure 7b) poorly connected to the perimeter walls, and pavement constituted by single layer wood plank resulting extremely flexible and unsuitable to transfer seismic actions. Sometimes, cane panels supporting a thin layer of plaster cover the beams (see Figure 7c). In other cases, there are steel beams with masonry vaults as showed in Figure 7d. Most of the buildings in category A1 have rectangular shape with openings aligned at the various floors. Generally, the partitions are irregular in plan and elevation.

As far as the building category A2 is concerned, a typical and representative example of isolated historical stable-hayloft is reported in Figure 8a-b. The need to achieve large volumes to store hay and wheat without introducing inner structural elements led to the adoption of long and high single leaf masonry walls 25-30cm thick. In other cases, masonry columns, with cross-section ranging from 40×40cm^2 to 70×70cm^2 were realized and infilled by single course (12-15cm thick) walls. The intermediate floor over the stable typically has masonry vaults supported by internal columns, as in Figure 8c. Instead, the roof has wooden trussed structure with two or four pitches. In several cases, along one façade, the building has a portico adopted, in the past, to store grain or to shelter the work tools (see Figure 8d). Due to the high slenderness of vertical walls and columns (the height/thickness ratio reach values higher than 20) and the large distance between masonry walls, the structure is expected to be very flexible. Moreover, as the ground floor plan view in Figure 8a underlines, the building results strongly asymmetric because of the presence of the stiff walls of the stable. Therefore, torsional effects are expected, inducing an increase in the displacement demand typically heavier on the elements of the flexible side [35]-[37] (in this case on the columns of the portico).

The category A3, according to the nomenclature adopted in this paper, includes the “barchessa” and “casella” structures. Even though a limited number of archetypes are nowadays present in the Emilia territory, they represent a typical vernacular construction with specific characteristics. In fact, in several cases, the original layout has been modified or enlarged in the years, while in other cases the historic building has been demolished and replaced with a more modern structure. Following the outcomes of surveys and literature [34], typically they are 4-6 meters high, with in plan dimensions of 6-10m and 15-20m (respectively for transverse and longitudinal direction). The small wall thickness (variable from 15 to 25cm) makes them very flexible. Two buildings in the A3 group were detected (i.e. bldg. # 11 and # 22 in Table 2 and Table 3). The “barchessa” appeared with its original features, while the “casella” was modified over the years: perimeter brickwork walls, poorly connected to the original columns, was erected to close the transverse façades and an intermediate floor was added to the building. Even for this category, the presence of perimeter walls just on some façades of the building could introduce non-negligible torsional effects. This aspect will be further commented in the following Section.

The most variegated category among those defined in this paper, is definitely A4, which collects a mixture of different buildings, having just one or, more seldom, two floors, typically built with very poor materials and technologies, since they were used for minor services (e.g. old water closet, cellar, depository, pigsty, henhouse and oven) sometimes built with demolition wastes. Usually, these buildings have limited dimensions (with in-plane edges from 3 to 5 m) and storey-height varying from 2 to 2.5 m. The roof is double or single-pitched, constituted by wooden beams and flat bricks (thick 2-3cm) sustaining the clay roof tiles.

Two or more bodies with common structural elements and coupled dynamic behaviour compose a significant number of buildings in the Emilia area hit by the earthquakes. The interaction between different bodies represents a further source of building damage and then the composed buildings were considered in a separate category ("B") from the isolated ones ("A"). The most widespread type of aggregation concerns house and stable-hayloft structures. The buildings typically were built in the same period, so they have a common internal wall.

The following section describes, for each building category, damage and collapses detected in the aftermath surveys carried out on the 22 rural structures investigated here. An overview of the most frequent damage mechanisms is reported in Table 4.

4. Damage and collapses to vernacular buildings

4.1 Damage to building category A1

The damage observed for buildings in category A1 (isolated dwellings) are typically mode II mechanisms (i.e. mechanism in the wall plane [38]) to bearing and partition walls, as depicted in Figure 9a-b. Due to limited length and height compared to thickness, the mode I failure wall mechanisms (i.e. out-of-plane overturning, horizontal and vertical out-of-plane flexure) were not observed, even if the connections between orthogonal walls are in general very poor, as showed by the cracks in Figure 9c. Most of the damage must be attributed to the poor material properties of the masonry [15], realized in many cases with irregular texture and poor strength mortar [13]. Moreover, the floor-wall connection is rather lacking since in many cases, it was observed the sliding of beams from the masonry walls (see Figure 7b), or even the failure, due to loss of support, as documented in Figure 9d. In few cases, also failure of lintels (see Figure 9e) or masonry arches (Figure 9f) have been observed, typically involving permanent settlements to the horizontal structures of the floors.

4.2 Damage to building category A2

Several damage affected the A2 category of the stable-hayloft buildings. In fact, many collapses or severe damage and consequent building demolition were detected for this category. The typical structural physiognomy makes the stable-hayloft extremely vulnerable to seismic actions. In fact, in general they are very asymmetric, due to the irregular wall layout; they have a flexible roof at the top and very slender vertical elements. The principal causes of stable-haylofts collapse are to ascribe to overturning of walls and vertical and horizontal out-of-plane flexure mechanisms. A catastrophic example of collapse for overturning, involving a whole façade from foundations to roof, is reported in Figure 10a. A similar scenario is showed in Figure 10b, but in this case, the out-of-plane flexure collapse anticipated the overturning façade because of the presence of some steel ties. Figure 10c shows the global collapse for horizontal flexure local mechanisms of another traditional stable-hayloft for out-of-plane horizontal flexure mechanism. Even if the behaviour of an existing masonry building subjected to moderate-strong earthquake is almost certainly nonlinear, the analysis of the elastic vibration modes of the structure could provide interesting information before severe damage or collapses occur [39]. As found in a wide literature review (see for example [40]-[43]), linear dynamic analysis of large masonry structures is always performed, prior to the application of more sophisticated approaches. In fact, linear analysis allows a quick preliminary assessment of the adequacy of the structural models before constructing more detailed models or local models of critical parts to be studied separately by means of more complex analyses [44]. In order to better understand the dynamic behaviour of a typical building of this category, the elastic finite element model (FEM) of the stable-hayloft showed in Figure 8, collapsed during the event of the May 29th, was realized. The global FEM is showed in Figure 11(a1). The walls in the FEM were modelled by means of 4-node Lagrangian shell elements. The masonry columns with elastic beams. For the masonry, elastic properties were selected the average values provided in [15] and obtained by the experimental in-situ tests. They were a Young modulus $E=2.6GPa$ and a Poisson ratio $\nu=0.25$. The rigid floor of the stable area has been realized by introducing a 5cm thick RC slab (measured during on-field survey). The model was clamped at the base. As far as the roof is concerned, beam finite elements were introduced in order to model the structural wooden members accurately considering the flexible behaviour of the roof diaphragm. The elements have the cross-section dimensions detected during the building survey and an elastic modulus $E= 8GPa$, typical for wood classes in the investigated region, was considered. The wooden elements were considered pinned-pinned at their extremities.

The study of the natural frequencies showed that first natural mode (with $T_1=0.54s$) having highest percentage of effective mass (around 32%) activates displacement in the longitudinal direction (i.e. along the longer building dimension) of the building, by inducing an out-of-plane flexure of the walls in the transverse direction (i.e. along the shorter building dimension). The deformed shape of first mode is showed in Figure 11(b1). As a further confirmation, the response spectral analyses provide peak roof displacements around 45mm, compatible with those assessed by the maps in Figure 5b for the area close to building #18. The principal stress contour depicted in the Figure 11(c1) highlights that maximum values (black colour) are expected along vertical edges of transverse walls. The estimated stress values abundantly overcome the masonry flexure strength [45], thus developing a vertical cylindrical plastic hinge that anticipated the activation of an out-of-plane flexure mechanism of the transverse walls producing the effects depicted in Figure 11(d). The accurate on-field inspection revealed that also the inner transverse walls collapsed, as assessed by the numerical model. This could be a reasonable, even though qualitative, explanation of the activation of the collapse mechanism. As a further attempt to explain the global collapse of the building as a series of partial local collapses, the authors investigated the behaviour of the building after the removal of the roof and collapsed walls, thus considering the updated FEM depicted in Figure 11(a2). Following an analogous procedure, it is worth to note that the updated model has a first natural mode, again with the highest percentage of vibrating mass (see Figure 11(b2)), involving the out-of-plane flexure behaviour of the perimeter longitudinal walls, portrayed in Figure 11(e), actually collapsed. Then, further higher vibrating modes predicted the failure of perimeter longitudinal walls on the other façade. As already stated, the adopted linear FEMs are not properly suitable to study (quantitatively) the behaviour of the building in a wide nonlinear range until collapse, however they can provide a first attempt for a reasonable (qualitatively) explanation of the building failure. In order to provide quantitatively results also in the nonlinear range the FEMs should be updated with the introduction of further hypotheses on a wide series of aspects, e.g. inelastic properties and behaviour of materials, behaviour of wall-wall and wall-roof beam connections, length of support before unseating of wooden beams, since other information are not available at present.

As the distance from the epicentre region increased, generally vertical walls did not collapse but the buildings reported severe damage to roof elements and, in some cases, the main wooden beams fell down. This can be probably attributed to beam-wall relative displacement, causing unseating and loss of support of horizontal elements. In fact, due to the building asymmetry, introduced e.g. by non-regular infills, non-symmetric walls, presence of portico and stable, two different vertical elements could vibrate in asynchronous way, by imposing at the extremities of horizontal beams, tensile force bigger than friction force and able to activate the sliding mechanism. This particular situation is showed in Figure 10d, with pitched-roof collapsed without any apparent damage to the vertical elements.

As already detected during the aftermath surveys on historical masonry buildings [46], the unrestrained forces of the beams of a deformable pitched-roof, excited by the ground motion component in the plane of the beams, can cause the overturning of a limited portion of masonry panels close to the roof. This local damage mechanism, typical of historical churches [47], has been detected in few cases also for historical stable-hayloft as depicted for instance in Figure 10e. In some cases (one of them is reported in Figure 10f) the slender columns bearing the hayloft roof reported severe damage conditions in the proximity of their base (i.e. the roof of the stable), because the horizontal seismic displacements at the building roof imposed a considerable rotation at the base-section where they are clamped, originating an uncommon “plastic hinge”.

The principal causes of collapse of this building category has to be ascribed to the high slenderness of the vertical walls or columns, coupled to the absence of a rigid floor diaphragm able to prevent the relative settlements between different vertical elements and avoid the sliding of roof beams from their seat. In some cases, the presence of steel ties avoids the overturning of the walls, but these devices were not sufficient to avoid the above-described catastrophic scenario.

4.3 Damage to building category A3

The “barchessa” and the “casella” building types represent a very particular feature of the historical vernacular building heritage of the Emilia area. In fact, this type of structure adopted in past to store hay or grain was very widespread over the region, due to its natural vocation to livestock farming and cereal cultivations. Currently, few original examples of these buildings exist in this area, due to their modification or demolition, and the recent earthquakes caused the loss of several of these vernacular architectural archetypes.

During on-field surveys, the authors detected a collapsed “barchessa” preserving its original features. The masonry building has dimensions around 8.20m×17.88m×5.10m (B×L×H, where B is the transverse in-plane dimension, L the longitudinal in-plane dimension, and H the average height of the building). Plan and longitudinal vertical view are reported in Figure 12a-b. The vertical walls are well connected and 25cm thick. The columns have $50\times50cm^2$ as gross-section. The collapse of the building is detailed in Figure 12c as it appeared few days after the May 29 earthquake. Similar to some stable-haylofts of category A2, due to large slenderness of vertical walls in absence of a rigid floor diaphragm, the out-of-plane flexure mechanism of a wall produced the complete collapse of the roof. With the aim of better understanding the dynamic properties of this class of buildings, two types of elastic FEMs have been adopted.

The first class of models, reproducing the whole geometry of building #22, is depicted in Figure 13. Three different assumptions, shown respectively in Figure 13a, b and c, have been made by considering alternatively an infinitely flexible floor, an infinitely rigid floor, and the real stiffness of the roof floor constituted by wooden beams. The walls were modelled by means of 4-node lagrangian shell elements. The masonry columns were elastic beams. For the masonry properties were selected the average values provided in [15]. They were a Young modulus E=2.6GPa and a Poisson ratio ν=0.26. The models were clamped at the base. As far as the case simulating the real roof stiffness is concerned, beam finite elements were introduced in order to model the structural wooden members. The wooden elements have the cross-section dimensions detected during the building survey and elastic modulus E= 8GPa. The wooden elements were considered pinned-pinned at their extremities.

The deformed shapes associated at the two natural periods having the highest percentage of effective mass in X and Y directions (where X is parallel to the longitudinal direction and Y is parallel to the transversal direction) are reported in the figure for the different hypotheses. As expected, the flexible floor provides the longer periods and the deformed shapes are the local vibrating modes of the various vertical elements with their tributary mass. The considerable in-plane asymmetry, for seismic action component along longitudinal direction, do not produce significant torsional effects, since the vibrating modes mainly imposed translational displacements. On the contrary, the seismic response for the case of rigid floor hypothesis (Figure 13b) show deformed shape imposing roof displacement mainly governed by torsional vibrating modes. In this case, the natural periods are generally shorter than the previous and they are associated to deformed shapes that change also the vibrating shape of local modes. It is worth to note that the behaviour of the FEM with real floor (Figure 13c), have deformed shapes and range periods more similar to those of the infinitely deformable floor FEM, thus indicating that typical trussed wooden elements constituting the floors of historical "barchessa" are very far from rigid floor assumptions. In general, the existent roof solution does not introduce significant torsional effects. By the prospective of a seismic strengthening, in the design of the upgrading interventions for this class of buildings, the introduction of a very stiff floor does not create evident benefits, while it could even cause a worse global dynamic behaviour of the building. It is important to highlight that the displacements assessed by means of dynamic response spectra analyses are completely different for the case of the rigid floor (maximum expected displacement of 1cm), while are comparable for the real and deformable floor assumptions (respectively 19 cm and 23 cm). These values are in good agreement with those provided by the spectra in Figure 3d (about 13-21cm following the records of MIR01 station for T_1=1.4s). In a first simplified modelling attempt, the deformable floor FEM provided a conservative displacements scenario.

Finally, due to the poor in-plane floor stiffness of the actual in-place wooden elements, local models of single vertical elements could be adopted in order to obtain an approximation of the vibrating periods involving element local modes.

With the main goal to obtain a realistic range of the first elastic vibrating periods of wall local modes for the structure in classes A2 and A3, a second class of FEMs was considered. The period value can result useful to achieve a rough, but very rapid, estimation of the maximum displacement that a structure could have experienced during the recent earthquakes (for example by considering the Figure 3c-d or Figure 5). The considered FEMs and the main results in terms of first out-of-plane vibrating periods are reported in Figure 14. In the work, two different types of walls (i.e. longitudinal and transverse) were considered, with two different constraints along the supported edges (i.e. cylindrically hinged and clamped) and for different pairs of H and L characterizing the walls (H: height; L: length). For H the most typical values equal to 4, 5 and 6m were considered; for L values of 15, 18 and 20m for longitudinal walls and 6, 8 and 10 for the transverse have been considered. The masonry walls thickness has been set equal to 25cm. Even in this case, the walls were modelled by means of 4-node lagrangian shell elements. with Young modulus E=2.6GPa and a Poisson ratio ν=0.26. The walls were restrained along three and two edges, respectively for longitudinal and transverse models (as showed by the deformed shape in Figure 14a). The Figure 14b, reporting the periods as a function of L/H ratio, shows that typical first vibrating periods of the vertical walls range from 0.2s to about 1.2s. The knowledge of the L/H ratio and the selected constraint condition, allows to evaluate the first vibrating period of a wall element, and the displacement experienced during the earthquake can be obtained from Figure 3c-d. The frequencies evaluated by the authors via FEM analyses were compared with the outcomes in [48] in order to check the validity of the models and their discretization. By the comparison on the first frequency, performed for the available L/H ratio, a maximum difference of 8% emerged, this value is widely acceptable for the scope of the work.

The “barchessa” studied in the present work has L/H ratio equal to 3.50 and 1.60 respectively for longitudinal and transverse walls. The comparison between vibrating periods of local and global models, shows that the most suitable restraint hypothesis for the walls is the one prescribing cylindrical hinge along the edges. In fact, the global models provide a vibrating period of 1.02s and 1.05s, respectively for vibrating modes involving local modes of longitudinal and transverse wall. The estimations of vibrating periods from local FEMs (with hinged edges) result very close to those correct, providing the Figure 14b values of 0.92s and 1.08s, respectively for longitudinal and transverse wall.

Due to reduced thickness, if compared to the other dimensions, the hinge restraint hypothesis may appear suitable for most of the structures in the categories A2 and A3. By means of the analysis of the displacements map of structures with first vibrating period around 1s, as the “barchessa” investigated here, the evaluation of the maximum displacements suffered during the event of May 29th provides values larger than 10cm for an epicentre distance of 15-20km (see Figure 5b2). This high seismic displacement demand could explain the overturning mechanisms observed in slender buildings, since in several cases it produced the exit of the vertical loads resultant from the wall base section.

The “casella” building, shown in Figure 12d, was modified from its original configuration over the years: the transverse (i.e. the shorter) façades were infilled by brickwork walls poorly connected to original corner columns, and an intermediate stiff floor was added. In this building, conversely to the “barchessa” response, the contemporary presence of strong asymmetry (for the presence of perimeter walls just on three out of four façades) and stiff intermediate floor probably magnified the torsion effects. In fact, Figure 12e shows the most important seismic-induced damage to the columns caused by the asymmetric behaviour of the building. Maybe due to torsion effects, the corner columns were literally cut at the level of the intermediate floor, and the residual settlements (of 2-3cm) highlighted in Figure 12e support this hypothesis. Furthermore, the lack of corner column-infill walls connections produced the detachment of the walls during the seismic events (see Figure 12f). The structure was demolished few months after the earthquake since was judged not reparable. The different dynamic response between the two buildings and the main reasons of their severe damage could have been completely different, but the consequences were catastrophic in both the buildings. In the hope of the authors, the indications emerging from this lesson learned would be of help to define the most suitable strengthening interventions for still standing buildings of the same category, which represent an important cultural heritage of that region.

4.4 Damage to building category A4

The typical damage to building category A4 are very similar to those observed for residential rural buildings of category A1, due to comparable geometries, but with amplified outcomes due to the poorer materials and construction techniques. In fact, as depicted for example in Figure 15a with regard to warehouse #14, the collapse of roof elements is one of the most recurring mechanisms, together with the in-plane failure of walls. Then, in many cases, the overturning of the infill panels non-adequately connected to vertical masonry columns was observed. An example is reported in Figure 15b. It shows a particular case of masonry infill collapse, where the bricks closing off the original openings were laid in their own plane, creating a panel extremely vulnerable to out-of-plane actions.

4.5 Damage to building category B

With reference to composed buildings (labelled as category B in this paper), it is worth to note that damage mechanisms observed during on-field inspections are very similar to those observed in isolated buildings, and the collapses can probably be ascribed to analogous causes. Moreover, few additional damage sources, to be attributed to the interaction between adjacent bodies, must be considered. In fact, due to the different use, the interacting bodies have often different storey level, inner height and wall slenderness, especially for building in category B1-2, mainly damaged by the 2012 earthquakes. As a result, in several situations, sliding and fall of roof beams (see Figure 16a), corner opening between non-properly connected orthogonal walls (see Figure 16b) were observed. Despite their slenderness (if measured on the hayloft side), sometimes the intermediate transverse walls reported X-shape cracks or bricks sliding typical of shear damage mechanism and did not collapse in local way because of the restraint guaranteed by intermediate storey on the other (i.e. home) side.

Among the observed seismic damage, it is worth to note those to non-structural elements. The failure or fall of these elements, even if non-responsible of building collapse, can represent a serious risk for people inside or nearby the building. In Figure 16c and d two typical examples are shown. The first is related to the failure of non-structural ornamental elements, like the "gelosie" (Figure 16c), holed infill walls typical of Northern Italy. The second refers to perimeter masonry cornice (Figure 16d), typically built with good external texture masonry, internally infilled by waste material with poor mechanical strength. Lastly, as mentioned above, in rural buildings it is not unusual to find porticos and wooden sheds commonly supported by thin masonry pillars. After the seismic events, some columns displayed cracking and damage at the base due to the large curvature prescribed in proximity of their connection to foundation elements. A typical crack pattern of the base portion is showed in Figure 16e. It is evident that the column base-section results partially no-longer working since it is detached by foundation plinth.

The presence on the Emilia territory of such a sensitive historical rural heritage to be preserved, calls for a suitable design strategy, based on the most effective technical solutions. Obviously, these solutions are not clearly identifiable if the actual vulnerability is not carefully understood and known. The catastrophic seismic damage and collapses described and detailed in the present paper should help to define the most suitable strengthening interventions aimed at reducing the sensitivity of historical vernacular buildings.

5. Conclusions

In this paper, damage and collapses collected during surveys on rural historical buildings in the aftermath of the 2012 Emilia earthquakes were presented and commented. In the area hit by the earthquakes, few recurrent building typologies were found, and buildings of the same typology showed similar damage mechanisms. Therefore, in order to define the most typical damage affecting the different building typologies, the 22 structures of the building stock were classified in different categories based on plan distribution and use of each building.

The main reason of the collapse of most of the vernacular buildings can be attributed to an incorrect design philosophy, typical of old construction techniques in non-seismic zones, considering only gravitational and wind loads. Moreover, old rural buildings typically represent low quality constructions built with poor construction techniques and materials. The most commonly observed collapses were walls local mechanism (i.e. single or complex overturning, horizontal or vertical flexure), and in some cases in-plane shear of flexure failure. In few cases, the presence of irregular distribution of the infill panels anticipated the failure. The failures must be ascribed to a lack of effective connections between orthogonal walls, poor connections between floor elements and walls, excessive flexibility of floor diaphragms. In many cases, the buildings were demolished because of the severe damage reported.

The still standing historical vernacular buildings nowadays represent a huge cultural heritage, preserving the architectural, environmental and social peculiar features of the Emilia landscape and history. The outcomes presented in this paper allowed identifying the building typologies most vulnerable to earthquakes and, from the lesson learned after recent seismic events, to plan the most effective planning strategies in order to increase the safety of historical rural constructions by means of adequate repair and conservation interventions.

Of course, the strengthening interventions will need to be specifically defined for each category. With specific reference to building categories A2 and A3, the most vulnerable as discussed in the paper, the authors think that the following actions could significantly improve their performance:

- upgrading the solidity of horizontal structures (floor and roof), without excessively increase the storey mass and stiffness;
- strengthening the connection between horizontal and vertical structures;
- increasing the thickness of structural walls and partitions, in order to reduce their slenderness;
- introduce further structural elements (walls or columns) in order to reduce the flexure span length of long and high walls (i.e. perimeter longitudinal walls);
- removing irregularities (both in-elevation and in-plane) caused by infill panels layout;
- strengthening flexure capacity of columns base-section (e.g. with FRCM or FRP interventions if is not mandatory to preserve the fair-face of masonry elements).

Funding

This research did not receive any specific grant from funding agencies in the public, commercial, or not-for-profit sectors.

References

[1] IESN (Italian Experimental Seismic Network). http://www.iesn.it (accessed 1.10.2018).

[2] ITACA (ITalian ACcelerometric Archive) version 2.0. http://itaca.mi.ingv.it (accessed 1.10.2018).

[3] Ricciardi A. I distretti industriali italiani: recenti tendenze evolutive. Sinergie 2013;91:21-58.

[4] Minghini F, Ongaretto E, Ligabue V, Savoia M, Tullini N. Observational failure analysis of precast buildings after the 2012 Emilia earthquakes. Earthquakes and Structures 2016, 11(2): 327-346.

[5] Belleri A, Brunesi E, Nascimbene R, Pagani M, Riva P. Seismic performance of precast industrial facilities following major earthquakes in the Italian territory. Journal of Performance of Constructed Facilities 2014;29(5):04014135.

[6] Bovo M, Savoia M. Numerical Simulation of Seismic-Induced Failure of a Precast Structure during the Emilia Earthquake. Journal of Performance of Constructed Facilities 2018;32(1):04017119.

[7] Cattari S, Degli Abbati S, Ferretti D, Lagomarsino S, Ottonelli D, Tralli A. Damage assessment of fortresses after the 2012 Emilia earthquake (Italy). Bull Earthq Eng 2013;doi:10.1007/s10518-013-9520-x

[8] Penna A, Morandi P, Rota M, Manzini CF, da Porto F, Magenes G. Performance of masonry buildings during the Emilia 2012 earthquake. Bull Earthq Eng. 2013; doi:10.1007/s10518-013-9496-6;

[9] Parisi F, Augenti N. Earthquake damages to cultural heritage constructions and simplified assessment of artworks. Engineering Failure Analysis 2013;34:735-760.

[10] Sorrentino L, Liberatore L, Liberatore D, Masiani R. The behaviour of vernacular buildings in the 2012 Emilia earthquakes. Bull Earthq Eng. 2013;doi:10.1007/s10518-013-9455-2.

[11] Cattari S, Abbati SD, Ferretti D, Lagomarsino S, Ottonelli D, Tralli A. The seismic behaviour of ancient masonry buildings after the earthquake in Emilia (Italy) on May 20th and 29th, 2012. Ingegneria Sismica 2012, 29(2-3):87-119.

[12] http://www.regione.emilia-romagna.it/terremoto (last accessed 1.10.2018).

[13] Galli E, Savoia M, Colla C, Ferretti D. Mechanical and mineralogical characterization of mortar in masonry buildings damaged by the 20-29th May earthquake in Emilia. Key Engineering Materials 2015. 624:379-386.

[14] Ferretti F, Ferracuti B, Mazzotti C, Savoia M. Destructive and minor destructive tests on masonry buildings: Experimental results and comparison between shear failure criteria.

Construction and Building Materials 2019. 199:12-29. doi.org/10.1016/j.conbuildmat.2018.11.246.

[15] Foppoli D. Inspections and NDT for the characterization of historical buildings after seismic events: 2012 Emilia earthquake. Proceedings of 10th International Conference on Structural Analysis of Historical Constructions − SAHC 2016, Leuven, Belgium, September 13-15.

[16] Marastoni D, Benedetti A, Pelà L, Pignagnoli G. Torque Penetrometric Test for the in-situ characterisation of historical mortars: fracture mechanics interpretation and experimental validation. Construction and Building Materials 2017; 157:509-520.

[17] Ortega J, Vasconcelos G, Rodrigues H, Correia M. Assessment of the influence of horizontal diaphragms on the seismic performance of vernacular buildings. Bull Earthquake Eng 2018;16:3871-3904. https://doi.org/10.1007/s10518-018-0318-8.

[18] Barros R; Rodrigues H; Varum H; Costa A, Correia M. Seismic Analysis of a Portuguese Vernacular Building. J. Archit. Eng. 2018;24(1):05017010.

[19] Ortega J, Vasconcelos G, Rodrigues H, Correia M. Assessment of the efficiency of traditional earthquake resistant techniques for vernacular architecture. Engineering Structures 2018;173:1–27.

[20] Ortega J, Vasconcelos G, Rodrigues H, Correia M., Lourenco PB. Traditional earthquake resistant techniques for vernacular architecture and local seismic cultures: A literature review. Journal of Cultural Heritage 2017;27:181–196.

[21] ISTAT (Italian National Institute for Statistics). 2011. 15° Censimento generale della popolazione. ISTAT, Roma, Italy. (In Italian).

[22] Carydis P, Castiglioni C, Lekkas E, Kostaki I, Lebesis N, Drei A. The Emilia Romagna, May 2012 earthquake sequence. The influence of the vertical earthquake component and related geoscientific and engineering aspects. Ingegneria Sismica 2012;29(2-3):31-58.

[23] INGV (Istituto Nazionale di Geofisica e Vulcanologia). http://shakemap.rm.ingv.it/shake/index.html (accessed 1.11.2018).

[24] Shrestha B. Vertical ground motions and its effect on engineering structures: a state-of-the-art review. In: Proceeding int semin hazard manag sustain dev, Kathmandu, Nepal; 29-30 November: 2009. http://dx.doi.org/10.13140/2.1.2863.6165.

[25] Grimaz S, Malisan P. Near field domain effects and their consideration in the international and Italian seismic codes. Boll Di Geofis Teor Ed Appl 2014;55:717–38. http://dx.doi.org/10.4430/bgta0130.

[26] Li S, Xie L. Progress and trend on near-field problems in civil engineering. Acta Seismol Sin 2007;20:105-14. http://dx.doi.org/10.1007/s11589-007-0105-0.].

[27] Bovo M, Savoia M. Evaluation of force fluctuations induced by vertical seismic component on reinforced concrete precast structures. Engineering Structures 2019;178:70-87. https://doi.org/10.1016/j.engstruct.2018.10.018.

[28] Priolo E, Romanelli M, Barnaba C, Mucciarelli M, Laurenzano G, Dall'Olio L, et al. The Ferrara thrust earthquakes of May-June 2012: preliminary site response analysis at the sites of the OGS temporary network. Ann Geophys 2012;2012(55):591-7.

[29] Gallipoli MR, Chiauzzi L, Stabile TA, Mucciarelli M, Masi A, Lizza C, et al. The role of site effects in the comparison between code provisions and the near field strong motion of the Emilia 2012 earthquakes. Bull Earthq Eng 2014;12:2211-30. http://dx.doi.org/10.1007/s10518-014-9628-7).

[30] Paul G. Somerville Engineering characterization of near fault ground motions URS Corporation, Pasadena, CA, USA. 2005 NZSEE Conference.

[31] Mavroeidis GP, Dong G, Papageorgiou AS. Near-fault ground motions, and the response of elastic and inelastic single-degree-of-freedom (SDOF) systems. Earthq Eng Struct Dyn 2004;33:1023-49.

[32] Liossatou E, Fardis MN. Residual displacements of RC structures as SDOF systems. Earthq Eng Struct Dyn. 2015;44(5):713-734.

[33] Maino E, Benni S, Torreggiani D, Barbaresi A, Tassinari P. A quantitative physiognomic analysis of contemporary farm buildings to improve awareness in rural planning. Transactions of the ASABE 2016;59(2):509-519.

[34] Ortolani M. La casa rurale nella pianura emiliana. Centro di studi per la geografia etnologica, Florence; 1953.

[35] Lucchini A, Monti G, Kunnath S. Seismic behavior of single-story asymmetric-plan buildings under uniaxial excitation. Earthquake Engng Struct Dyn 2009;38:1053-1070.

[36] Perus I, Fajfar P. On the inelastic torsional response of single-storey structures under bi-axial excitation. Earthquake Engineering and Structural Dynamics 2005;34(8):931–941.

[37] Ghersi A, Rossi P. Influence of bi-directional ground motions on the inelastic response of one-storey in-plan irregular structures. Engineering Structures 2001;23(6):579–591.

[38] Tomazevic M.. Earthquake - resistant design of masonry buildings. Imperial College Press, London; 2000.

[39] Roca P, Cervera M, Gariup G, Pelà L. Structural Analysis of Masonry Historical Constructions. Classical and Advanced Approaches Arch Comput Methods Eng 2010;17: 299-325.

[40] Cardoso R, Lopes M, Bento R. Seismic evaluation of old masonry buildings. Part I: Method description and application to a case-study. Engineering Structures 2005;27: 2024-2035.

[41] Mistler M, Butenweg C, Meskouris K. Modelling methods of historic masonry buildings under seismic excitation. J Seismol 2006;10:497-510.

[42] Ramos LF, Lourenco PB. Modeling and vulnerability of historical city centers in seismic areas: a case study in Lisbon. Engineering Structures 2004;26:1295-1310.

[43] Milani G. Lesson learned after the Emilia-Romagna, Italy, 20-29 May 2012 earthquakes: A limit analysis insight on three masonry churches. Engineering Failure Analysis 2013;34:761-778.

[44] Meli R, Peña F. On elastic models for evaluation of the seismic vulnerability of masonry churches. In: Structural analysis of historical constructions. (SAHC) 2004; Balkema, Leiden, pp. 1121-1131

[45] ANTC (Aggiornamento delle Norme Tecniche per le Costruzioni) Italian Building Code. Ministerial Decree 17/01/2018. In Italian.

[46] Lagomarsino S. On the vulnerability assessment of monumental buildings. Bull Earthquake Eng 2006;4(4): 445-463.

[47] Lagomarsino S. Damage assessment of churches after L'Aquila earthquake (2009). Bull Earthquake Eng 2012;10:73-92. doi:10.1007/s10518-011-9307-x.

[48] Theory and Analysis of Elastic Plates and Shells. J. N. Reddy. CRC Press. 2nd Edition . First Published 2006.

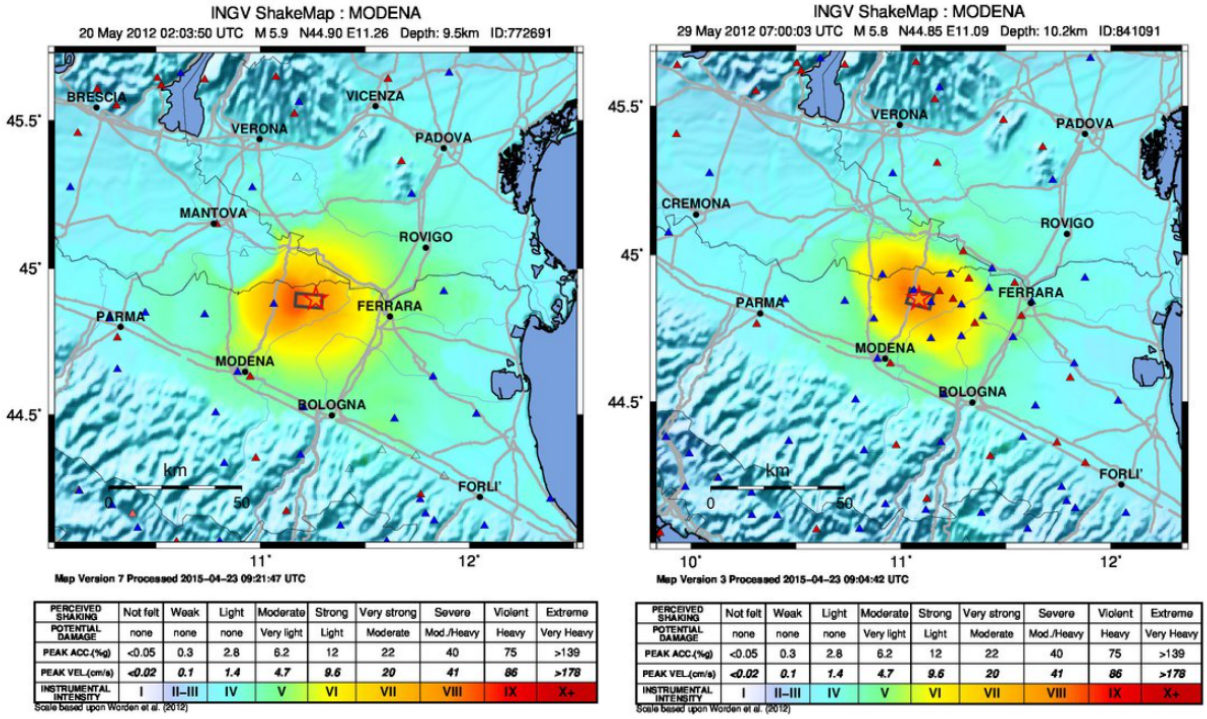

(a) (b)

Figure 1. Shake map of main shocks showing the PGA of the Emilia sequence for (a) May 20 and May 29 earthquake respectively (source [2]).

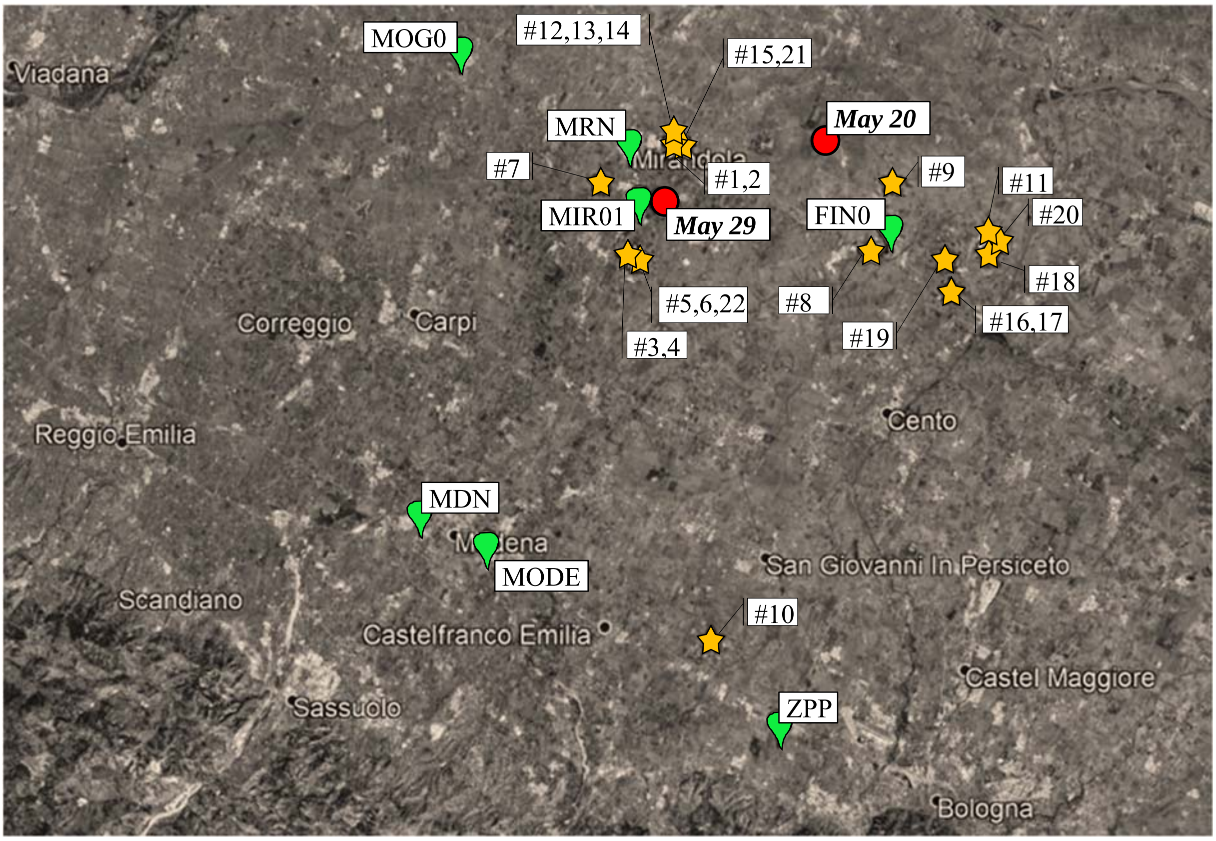

Figure 2. Position of seismic stations (green markers) and buildings studied in this paper (numbered yellow stars), with the location of epicentres of May 20 and May 29 ground motions (red circles).

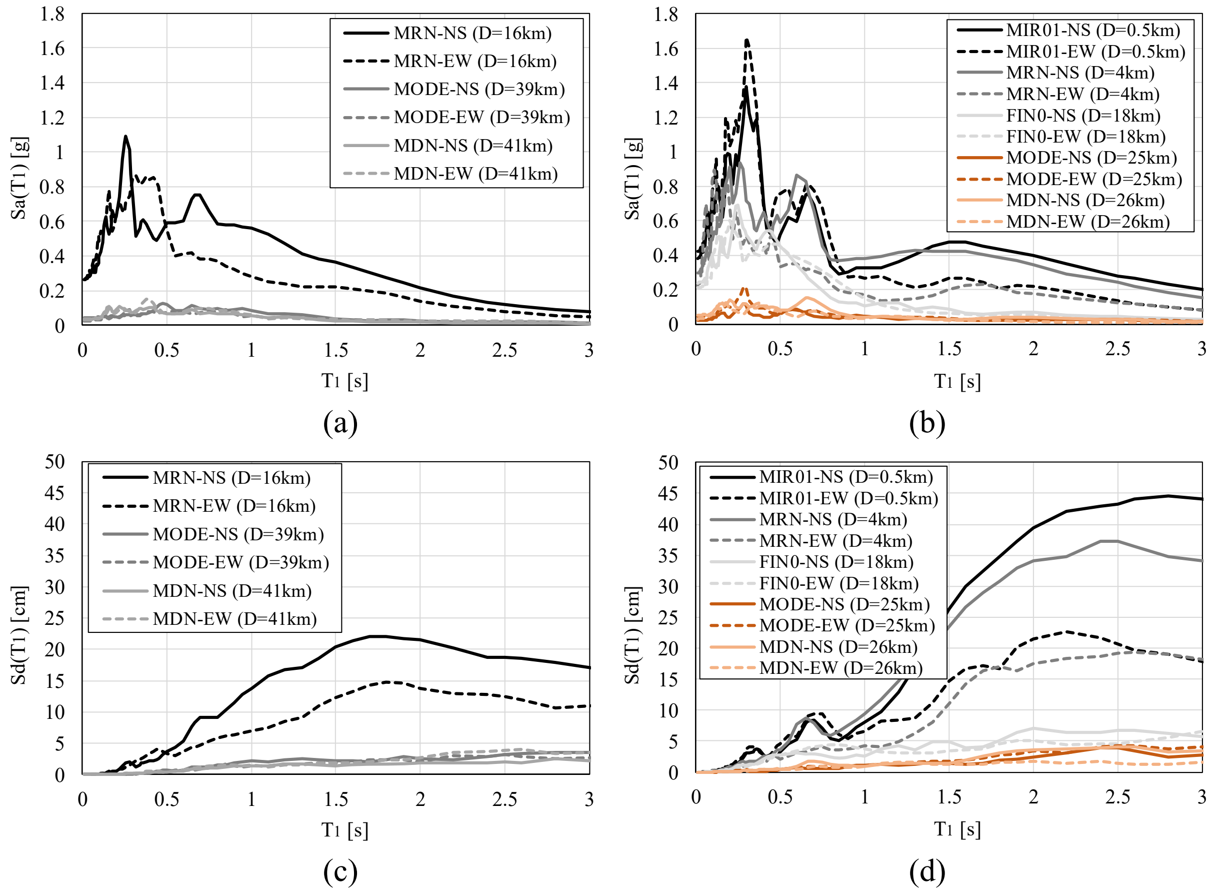

Figure 3. Response spectra 5%-damped of both the two (i.e. North-South and East-West) horizontal components of the ground motions for accelerometric stations closest to the epicentres. Pseudo-acceleration for events of the (a) May 20 and (b) May 29 earthquakes and pseudo-displacement for events of the (c) May 20 and (d) May 29. See Fig. 3 for station locations.

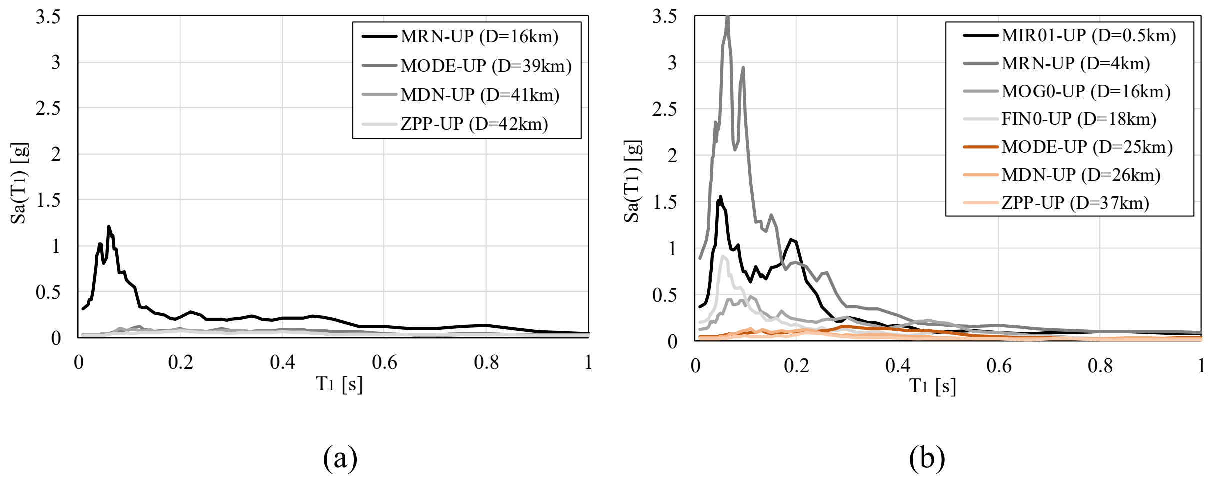

Figure 4. Pseudo-acceleration response spectra 5%-damped of the vertical components of the ground motions for accelerometric stations closest to the epicentres of the (a) May 20 and (b) May 29 earthquakes.

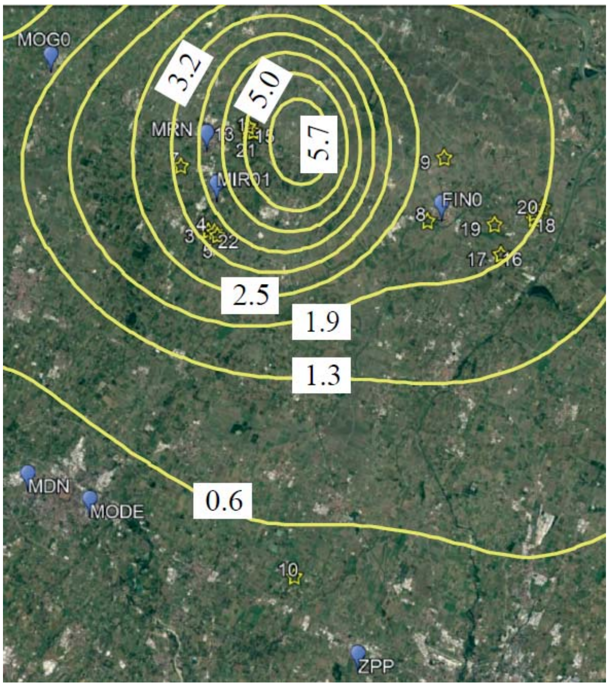

(a1)

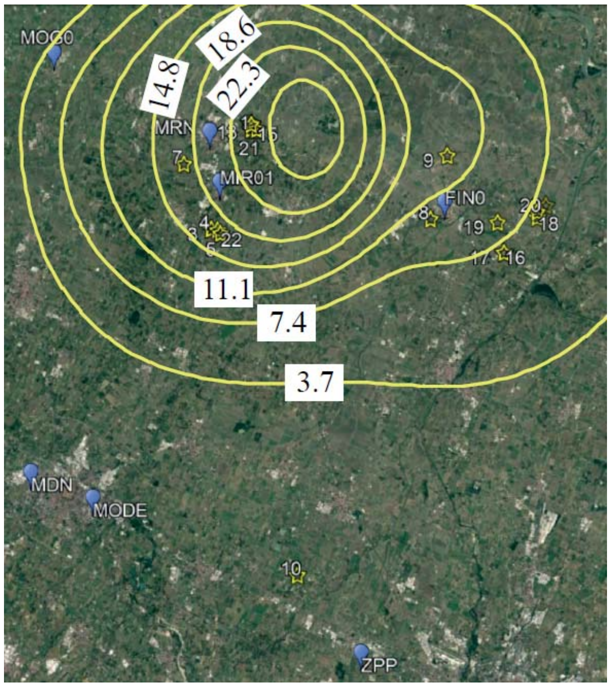

(a2)

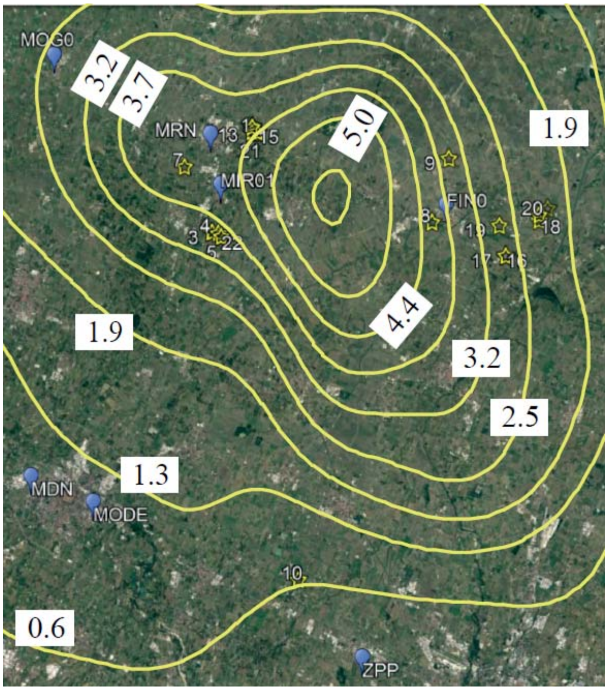

(b1)

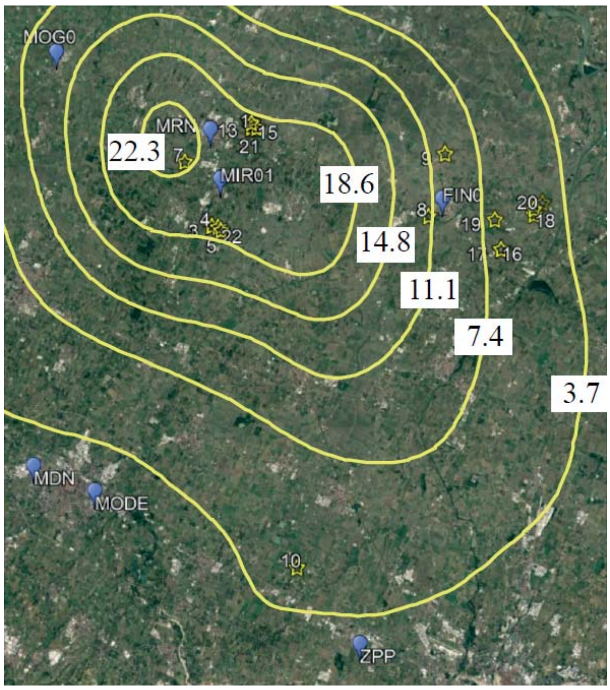

(b2)

Figure 5. Map of the horizontal displacement attenuation (expressed in cm) assessed for the earthquakes of May 20 for an elastic SDOF system with period (a1) 0.3s and (a2) 1.0s and May 29 for an elastic SDOF system with period (b1) 0.3s and (b2) 1.0s.

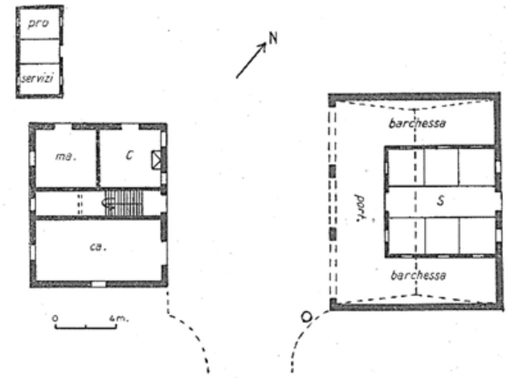

(a)

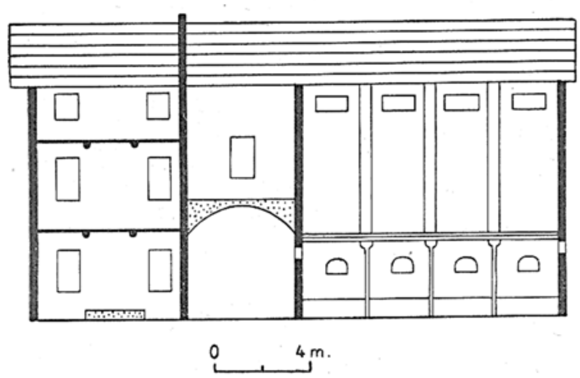

(b)

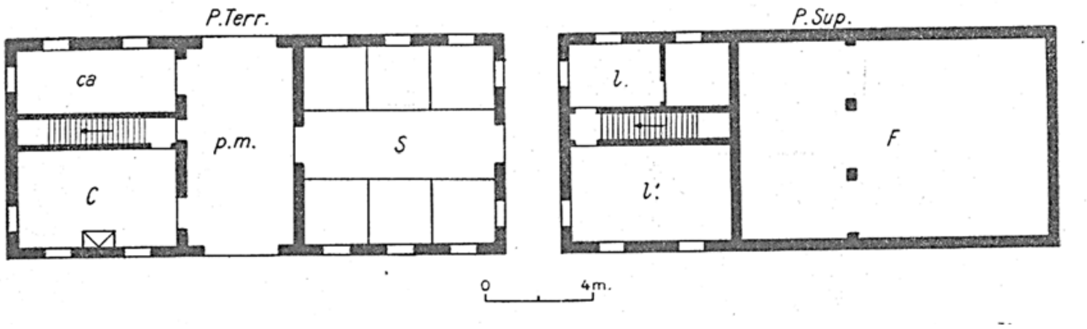

(c)

Figure 6. Historical documentation on rural buildings in the Emilia region as extracted by Ortolani [34]. (a) Plan view of typical rural courtyard in the area of Modena. (b) Vertical section and (c) plan view of ground (left) and first (right) floor of typical building with “porta morta” element between stable-hayloft and dwelling. In the figure the symbols means: C: cucina=kitchen; ca: cantina=basement; ma: magazzino=warehouse; port: portico; p.m.: “porta morta”; S: stalla=stable; l: camera da letto=bedroom; F: fienile=hayloft.

(a)

(b)

(c) (d)

Figure 7. Details on materials and construction techniques of historical rural buildings. (a) Different masonry wall texture. (b) Structure of a wooden floor; (c) Cane panels protecting timber beams. (d) Vaulted masonry floor.

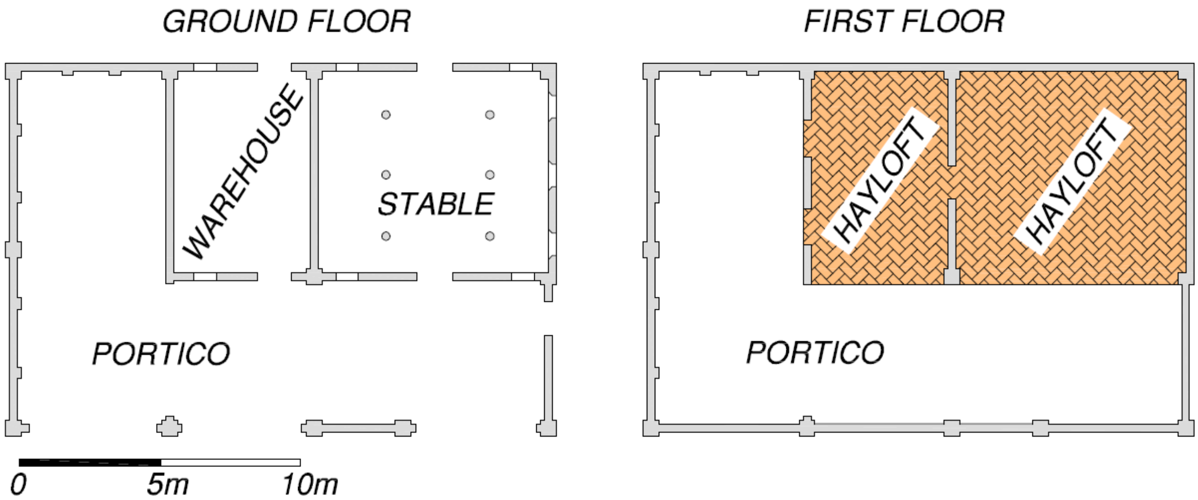

(a)

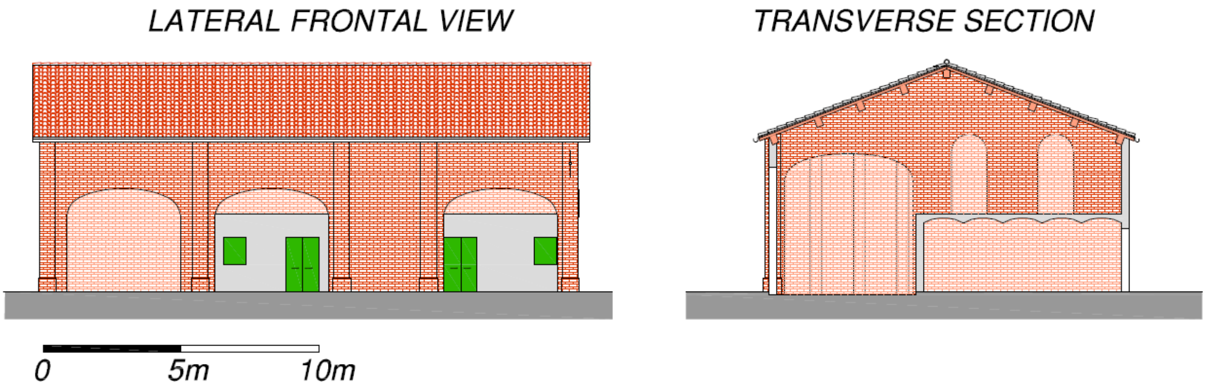

(b)

(c)

(d)

Figure 8. Typical stable-hayloft building (bldg. #18). (a) Plan view of ground and first floor; (b) Lateral view and transverse section; (c) Inner view of stable. (d) External view of a portico of a stable-hayloft supported by slender masonry columns (the structure elements did not report damage during the seismic sequence).


(a1)


(a2)

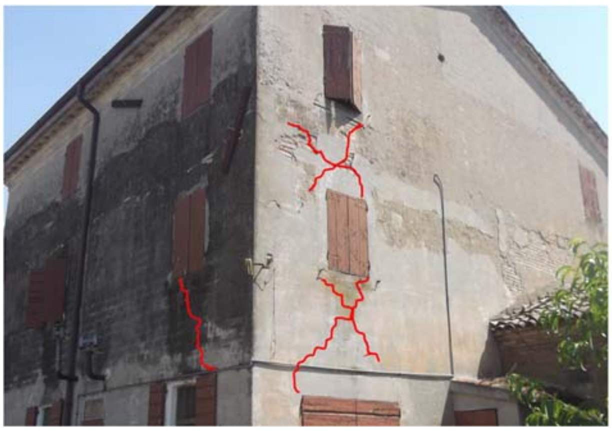
(b1)


(b2)


(c)


(d)

(e) (f)

Figure 9. Main damage to building category A1. Example of in-plane damage induced by seismic force on (a) partition walls (bldgs. #2 and #3) and (b) bearing walls (bldgs. #6 and #3); (c) Cracking of corner between two orthogonal masonry walls (bldg. #1); (d) Loss of support of a wood beams from the masonry walls (bldg. #2); (e) View of a lintel failed and (f) arch collapse (bldg. #20).


(a) (b)


(c) (d)


(e) (f)

Figure 10. Main damage to building group A2. Example of catastrophic stable-hayloft collapses for (a) overturning of the façade (bldg. #1), (b) out-of-plane vertical flexure (bldg. #18), and (c) horizontal flexure mechanism (bldg. #10). (d) Loss of support of the roof beams for the excessive deformations of the building (bldg. #4). (e) Overturning of a limited portion of masonry panels for the horizontal force transmitted by the beam elements of a flexible roof (bldg. #1). (f) Severe damage on a slender masonry column (bldg. #4).

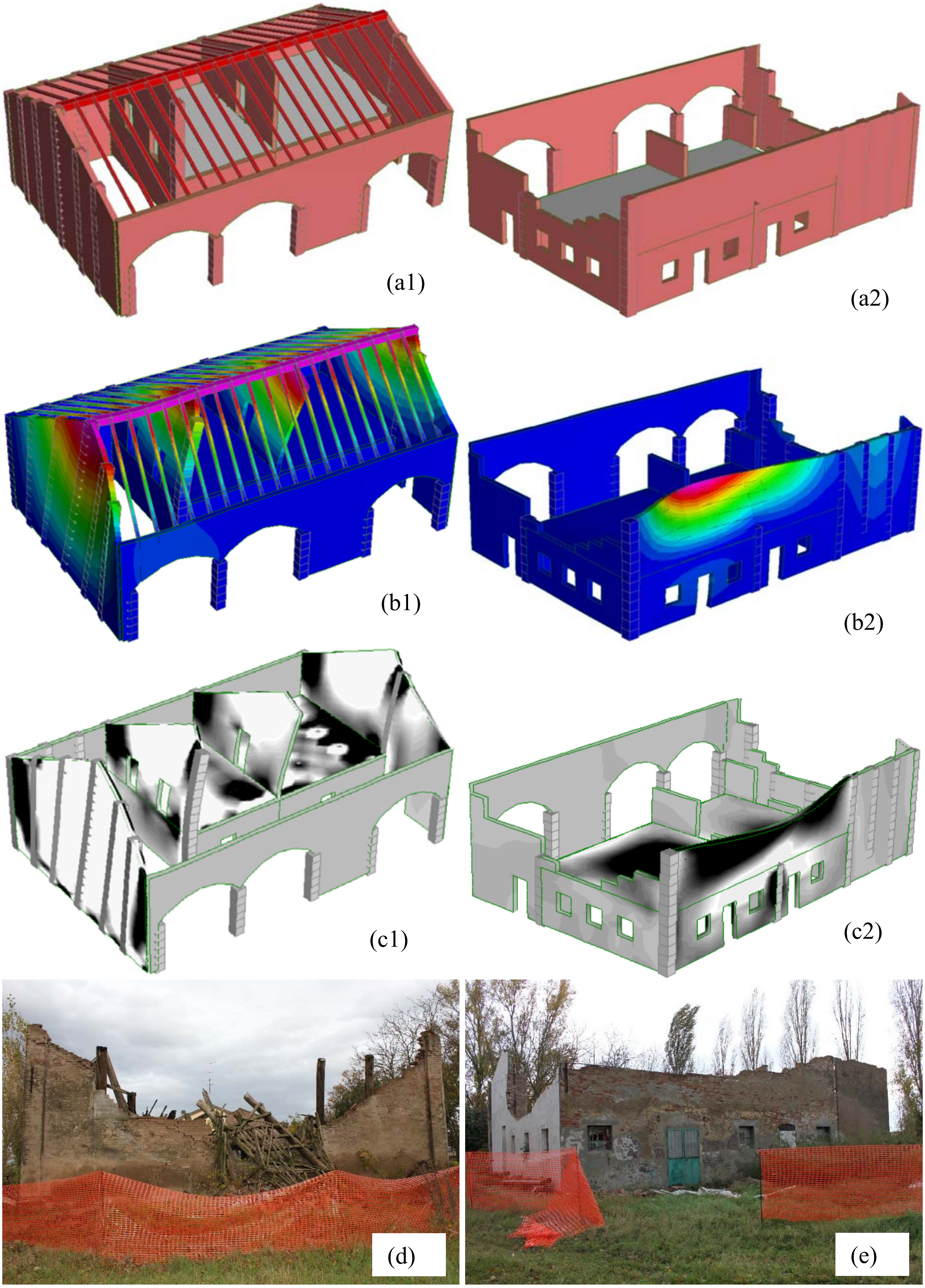

Figure 11. Comparison between observed damage and numerical assessment on building #18. (a) Finite element models; (b) Deformed shape of the first natural vibrating mode; (c) Principal stress contour on masonry walls. (1) Original structure; (2) Model updating after the collapse of some walls. (d) Detail of wall collapse along transverse and (e) longitudinal direction.

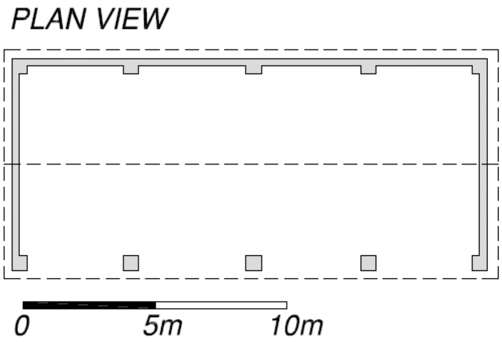

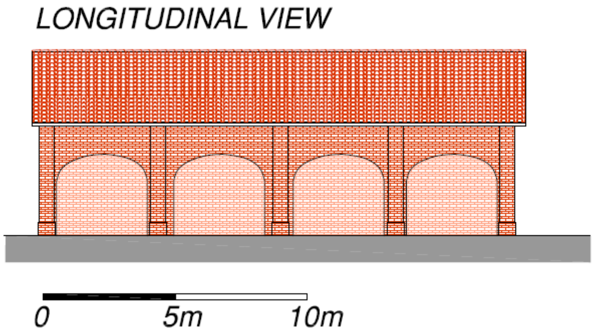

(a) (b)


(c) (d)


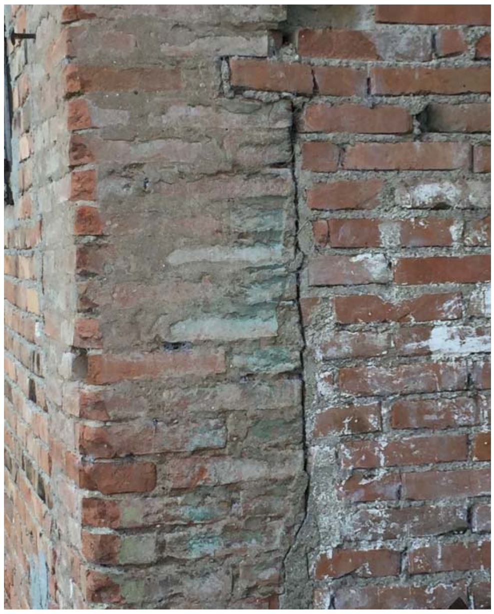

(e) (f)

Figure 12. Main damage to buildings of category A3. (a) Plan view, (b) lateral view and (c) collapse scenario of a “barchessa” building (bldg. #22); (d) Lateral view of a “casella” (bldg. #11) with details of severe damage to (e) masonry columns due to excessive shear force imposed by torsion and (f) infill walls for detachment from the bearing columns.

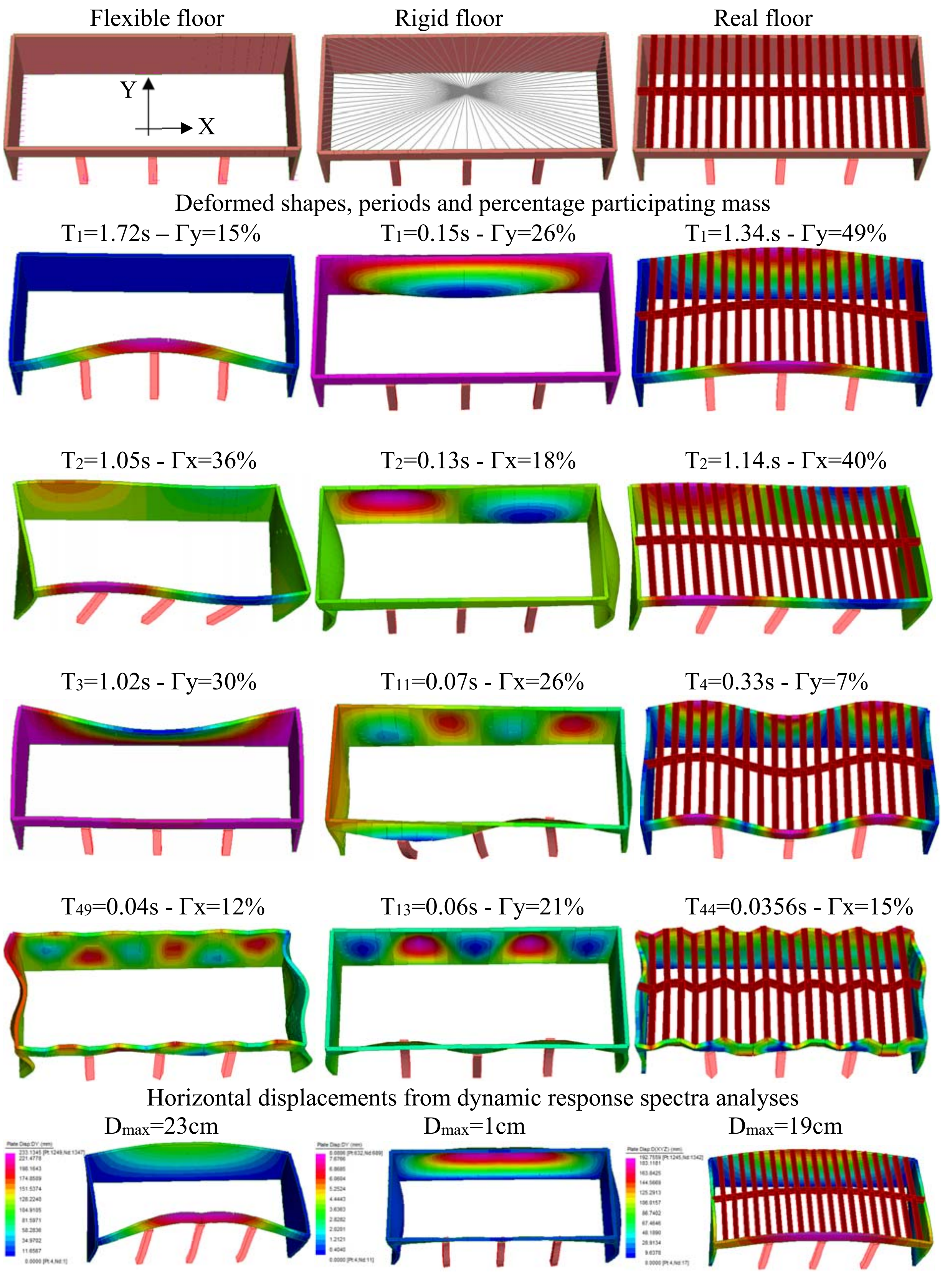

(a) (b) (c)

Figure 13. Finite element modelling of building #22. Deformed shapes, vibrating period (T), percentage participating mass (Γ), and displacement demand in the hypothesis of (a) flexible floor, (b) rigid floor and (c) real floor.

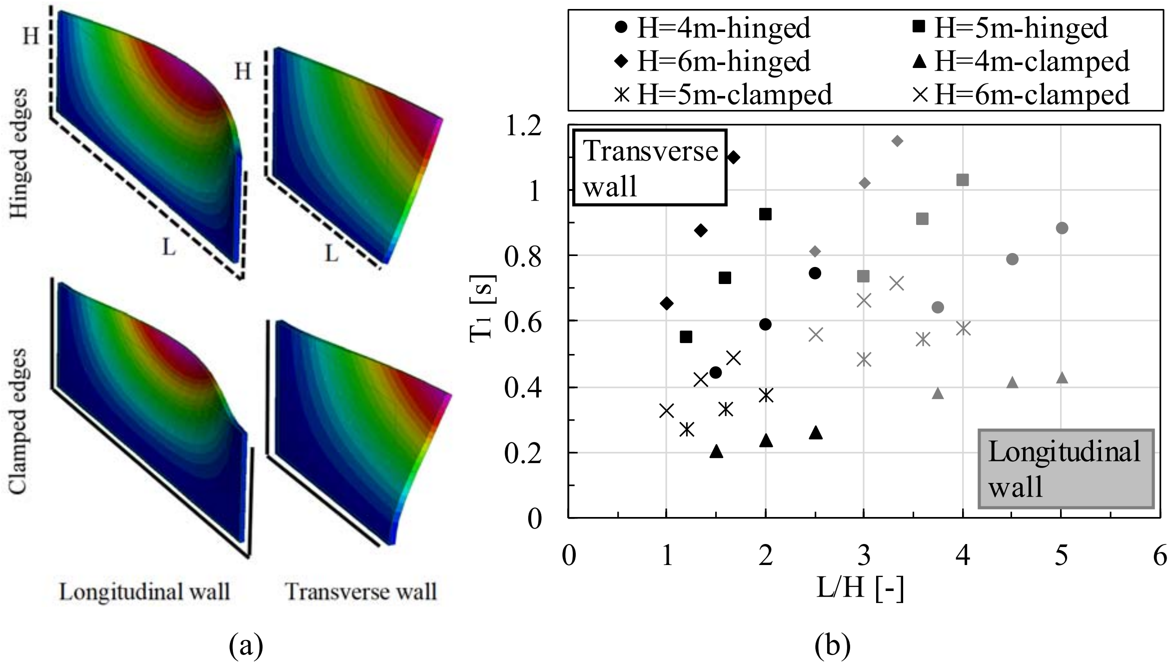

Figure 14. Analysis of the first vibrating periods of vertical walls in buildings with flexible floor. (a) Finite element modelling and deformed shape for different types of restraint; (b) first out-of-plane vibrating periods as a function of the L/H ratio, with L and H as reported in figure.

(a1)

(b1) (b2)

Figure 15. Main damage to buildings of category A4. Example of (a1-a2) structure collapse with loss of support of the roof structures (bldg. #21 and #14) and (b) overturning of masonry infill walls due to the erroneous arrangement of the bricks (bldg. #17). Picture (b2) shows the activation of the overturning mechanism but with no fall of the panel.

Figure 16. Detail of damage to category B buildings and non-structural elements. (a) Fall of timber roof beams from the intermediate wall in the composed bldg. # 8. (b) Shear cracks on a wall (bldg. #8). (c) Failure of “gelosie”, typical holed infill walls (bldg. #5). (d) Fall of a portion of the perimeter masonry cornice (bldg. #5). (e) Cracking at the base of a masonry column portico (bldg. #7); (f) Internal and (g) external view of the detachment of the infill panels from the bearing columns due to a poor connection (bldg. #12).

Station code	Station name	Lat. [°]	Long. [°]	May 20th			May 29th		
				D[†] [km]	PGA_H[‡] [cm/s^2]	PGA_V[§] [cm/s^2]	D[†] [km]	PGA_H[‡] [cm/s^2]	PGA_V[§] [cm/s^2]
MIR01	Medolla	44.84	11.07	-	-	-	0.5	411.37	361.54
MRN	Mirandola	44.87	11.06	16.1	258.80	297.30	4.1	288.63	840.74
MOG0	Moglia	44.93	10.91	-	-	-	15.8	235.62	124.18
FIN0	Finale Emilia	44.82	11.28	-	-	-	17.5	234.28	189.07
MODE	Modena	44.62	10.94	38.6	41.85	32.66	25.3	44.09	42.34
MDN	Modena 1	44.64	10.88	40.5	36.24	28.67	25.7	50.53	35.14
ZPP	Zola Predosa Piana	44.52	11.20	41.5	22.81	19.66	36.9	20.77	22.31

[†] Distance from epicentre
[‡] Horizontal Peak Ground Acceleration
[§] Vertical Peak Ground Acceleration

Table 1. Main information recorded by representative accelerometric stations close to epicentres during the two main shocks of 2012.

Bldg. #	Bldg. category	Lat. [°N]	Long. [°E]	D_{20}[†] [km]	D_{29}[‡] [km]	Notes and building use
1	A2	44.892	11.102	10.13	4.75	Stable-hayloft
2	A1	44.895	11.101	10.13	4.76	Residential dwelling
3	A1	44.824	11.064	15.04	3.54	Residential dwelling
4	A2	44.825	11.063	15.05	3.54	Stable-hayloft
5	B1-2	44.823	11.069	14.69	3.36	House adjacent to stable-hayloft
6	A1	44.821	11.072	14.64	3.50	Residential dwelling
7	B1-2	44.869	11.037	15.43	4.68	House adjacent to stable-hayloft
8	B1-2	44.831	11.273	7.45	14.66	House adjacent to stable-hayloft
9	A4	44.873	11.289	5.08	16.01	Warehouse
10	A2	44.589	11.144	34.07	29.27	Stable-hayloft
11	A3	44.839	11.383	13.40	23.26	Originally "casella" than infilled on transverse sides
12	B1-2	44.896	11.102	10.11	5.14	House adjacent to stable-hayloft
13	A4	44.895	11.102	10.11	5.12	Pigsty
14	A4	44.896	11.102	10.09	5.14	Warehouse
15	A1	44.892	11.107	9.70	4.85	Residential dwelling
16	B1-4	44.807	11.344	12.83	20.60	House between warehouse and vernacular chapel
17	A4	44.807	11.343	12.83	20.60	Warehouse
18	A2	44.831	11.376	13.24	22.69	Stable-hayloft
19	A1	44.828	11.338	10.96	19.73	Residential dwelling
20	A1	44.834	11.376	13.04	22.64	Residential dwelling
21	A4	44.892	11.107	9.80	4.84	Warehouse-garage
22	A3	44.821	11.072	14.63	3.48	"Barchessa"

[†] Distance from epicentre of May 20th
[‡] Distance from epicentre of May 29th

Table 2. Main information on the building stock collected during the aftermath surveys.

Bldg. #	Plan dimensions (m)	Number of floors	Max height (m)	Floors materials-techniques	Roof materials-techniques	Walls materials-techniques
1	20.7×17.0	2	11.1	Steel beams with vaulted holed bricks	Main+secondary timber beams	Fired bricks t=30cm
2	18.5×11.4	3	10.3	Timber beams	Main+secondary timber beams	Fired bricks t=30cm
3	15.2×11.2	3	7.90	Timber beams	Main+secondary timber beams	Fired bricks t=30cm
4	19.9×16.6	2	9.70	Steel beams with vaulted holed bricks	Main+secondary timber beams	Raw bricks t=30cm
5	13.5×29.7	2/3	10.70/ 11.50	Main+secondary timber beams/ Vaulted floor with RC slab	Main+secondary timber beams	Fired bricks t=30cm
6	9.10×19.0	3	9.70	RC beams with holed bricks	Main+secondary timber beams	Fired bricks t=30cm
7	35.3×9.10	3/2	8.30/ 8.20	RC beams with holed bricks / Steel beams with vaulted holed bricks	Main+secondary timber beams	Fired bricks t=35cm/ Fired bricks t=30cm
8	21.43×18.27	2/2	8.30/ 9.75	RC beams with holed bricks	Main+secondary timber beams	Raw bricks t=30cm
9	6.50×17.6	2	8.90	RC beams with holed bricks	RC beams with holed bricks	Raw bricks t=30cm
10	16.6×14.0	2	9.30	RC slab	Main+secondary timber beams	Fired bricks t=30cm
11	8.70×5.30	1	6.40	-	Main+secondary timber beams	Fired bricks t=25cm
12	12.2×21.0	2/2	10.4/ 10.9	RC beams with holed bricks/ Steel beams with vaulted holed bricks	Main+secondary timber beams	Fired bricks t=30cm/ Fired bricks t=30m
13	6.15×8.05	1	3.80	-	Timber beams	Fired bricks t=25m
14	14.0×6.90	2	7.25	RC beams with holed bricks	Main+secondary timber beams	Fired bricks t=15m
15	25.0×10.8	3	8.20	Main+secondary timber beams	Main+secondary timber beams	Fired bricks t=30m
16	14.6×8.60	2	7.90	RC beams with holed bricks	Main+secondary timber beams	Fired bricks t=30m
17	12.9×3.40	2	5.10	Timber beams	Main+secondary timber beams	Raw bricks t=25cm
18	15.3×13.5	2	8.20	Steel beams with vaulted holed bricks	Main+secondary timber beams	Fired bricks t=25cm
19	13.7×12.3	2	8.00	Main+secondary timber beams	Main+secondary timber beams	Fired bricks t=30m
20	15.5×5.40	3	7.90	RC beams with holed bricks	Main+secondary timber beams	Fired bricks t=30m
21	19.6×13.3	2	7.30	Timber beams	Main+secondary timber beams	Fired bricks t=30m
22	8.20×5.15	1	6.60	-	Main+secondary timber beams	Fired bricks t=25m

Table 3. Main geometrical/materials information on the building stock collected during the surveys, where: RC: reinforced concrete.

Rural building category	Damage / Collapse mechanisms	Building #	Deficiencies / Causes
A (isolated building)			
A1 (dwelling)	DAMAGE - cracks for in-plane wall flexure - X cracks for in-plane wall shear - wall-wall corner cracks - cracks on partition walls - floor beams sliding COLLAPSE: - floor beams fall down - lintels / arches	 3,6,20 2,15,19,20 2,3,6 2,3,6,15 2,3,6,19 2 20,3,6	- flexible interstorey diaphragm - flexible roof - lacking floor-wall connections - lacking wall-wall connections - poor materials strength
A2 (stable-hayloft)	DAMAGE: - floor beams sliding - wall cracks COLLAPSE: - wall overturning l. m.[†] - out-of-plane wall flexure l. m.[†] - flexure-shear columns failure - roof beams fall down	 1,4,10 1,4,18 1 10,18 1,4 1,4,18	- flexible roof - slender walls - distance between vertical walls - lacking roof-wall connections - lacking wall-wall connections - in-plane asymmetry - non-regular infills - in-elevation irregularity
A3 (barchessa and casella)	DAMAGE: - permanent settings - cracks on column-infills connections COLLAPSE: - out-of-plane wall flexure l. m.[†] - roof beams fall down	 11 11 22 22	- flexible roof - slender walls/columns - lacking roof-wall connections - in-plane asymmetry - non-regular infills
A4 (minor services building)	DAMAGE: - cracks for in-plane wall flexure - X cracks for in-plane wall shear - cracks on infills/partitions COLLAPSE: - roof beams fall down - overturning of infills	 9,13 13,14 13,14,17 9,13 9,17	- flexible roof - lacking roof-wall connections - non-regular infills - poor materials strength
B (composed building)			
B1-2 (dwelling-stable-hayloft)	DAMAGE: - X cracks for in-plane wall shear - wall-wall corner cracks - cracks on partition walls - floor beams sliding - base column cracks COLLAPSE: - floor/roof beams fall down - infills failure - cornice fall down	 8,12 5,8,12 7,8,12 8,12 7 5,8 5 5	- same as for A1 - same as for A2 - interaction between adjacent bodies
B1-4 (dwelling-minor services)	DAMAGE: - wall-wall corner cracks - cracks on partition walls COLLAPSE: (Not observed)	 16 16	- same as for A1 - interaction between adjacent bodies

[†] l. m. : local mechanism

Table 4. Summary of the main damage and collapse mechanisms observed for the various rural building categories.